

Infrared spectroscopy and ellipsometry of magnetic metamaterials

W.J. Padilla¹, Ta Jen Yen², N. Fang², D.C. Vier³, David R. Smith⁴, J.B. Pendry⁵, X. Zhang², D.N. Basov³

¹Los Alamos National Laboratory, MS K764 MST-10, Los Alamos, NM 87545.

²Department of Mechanical and Aerospace Engineering, University of California at Los Angeles, 420 Westwood Plaza, Los Angeles, CA 90095.

³Department of Physics, University of California San Diego, La Jolla, California 92093-0319.

⁴Department of Electrical & Computer Engineering, Durham, NC 27708-0291.

⁵Condensed Matter Theory Group, Blackett Laboratory, Imperial College, London SW7 2AZ, UK.

ABSTRACT

We present S and P polarized measurements of artificial bianisotropic magnetic metamaterials with resonant behavior at infrared frequencies. These metamaterials consist of an array of micron sized ($\sim 40\mu\text{m}$) copper rings fabricated upon a quartz substrate. Simulation of the reflectance is obtained through a combination of electromagnetic eigenmode simulation and Jones matrix analysis, and we find excellent agreement with the experimental data. It is shown that although the artificial magnetic materials do indeed exhibit a magnetic response, care must be taken to avoid an undesirable electric dipole resonance, due to lack of reflection symmetry in one orientation. The effects of bianisotropy on negative index are detailed and shown to be beneficial for certain configurations of the material parameters.

Keywords: THz, meta material, left handed, negative index, bianisotropy, chiral, ellipsometry

1. INTRODUCTION

Recently the field of electromagnetism has seen significant excitement and rapid growth, due the discovery of left-handed metamaterials.ⁱ These artificially constructed materials are capable of achieving simultaneous values of negative electric ($\epsilon < 0$) and negative magnetic ($\mu < 0$) response, a feat that is difficult or impossible to achieve with naturally occurring materials. Although this behavior was predicted in 1967 by Veselago,ⁱⁱ his work was largely unknown until re-discovered and demonstrated by Smith et al. [i] in 2000. This previously unseen exotic electromagnetic response was termed “left-handed” due to the unique property that the wave number k lies along the direction of $-\mathbf{E} \times \mathbf{B}$, where \mathbf{E} is the electric field and \mathbf{B} is the magnetic field, thus following a “left-hand” rule. Although in 1967 “left-handed” may have been acceptable vernacular, we adopt the terminology negative index media (NIM) to describe a material with simultaneous negative values of ϵ and μ , to avoid confusion with the typical modern parlance reserved for describing chiral materials.

The critical component responsible for demonstration of NIM has been extended to work at terahertz (THz) frequencies.ⁱⁱⁱ This key element, termed a split ring resonator (SRR)^{iv} pictured in Figure 1, exhibits a resonant response to the magnetic component of an incident time varying electromagnetic field and is characterized by an effective magnetic permeability $\mu_{\text{eff}}(\omega)$. The demonstration of this high frequency artificial material shows that the concept of a magnetic response from non-magnetic conducting elements scales over an extremely broad range of frequencies, from RF^v and microwaveⁱ on the low end, to THzⁱⁱⁱ on the high end. There is much interest in extending these phenomena to optical frequencies owing to the exciting potential applications.^{vi} However, it is not known if the SRR structure will work at arbitrarily high frequencies.

In particular it is expected that there is some high frequency cutoff at which the utilization of SRRs as a magnetic material must cease. This is due to the fact that the magnetic response depends upon conducting elements. There is a

lack of bulk conductivity of metals as their dimensions are scaled to nano sizes, due to the ever decreasing wavelengths associated with the incident radiation. Moreover typical plasma frequencies for metals occur in the ultra violet, thus inducing insulating behavior. It is of great interest to determine the highest frequency at which SRRs may be utilized for negative index media and other future devices. Although as mentioned, high frequency magnetic response has been shown, it has not been directly demonstrated that the permeability obtains negative values. Thus negative index is still restricted to microwave frequencies.

Perhaps more importantly SRRs and other artificial structures utilized to obtain magnetic response are bianisotropic. A full characterization of their properties may thus require the measurement of four or more complex quantities. This presents a challenge even at microwave frequencies where S-parameter (complex reflection and transmission) measurements are common. At THz and higher frequencies this is more difficult and typically ellipsometry, or THz time domain spectroscopy are relied upon to obtain the real and imaginary portions of the response function. The utilization of artificial magnetic materials at THz and higher frequencies will thus greatly rely upon a full characterization of not only their frequency dependent electric and magnetic response, but also the inherent exotic properties that emerge for bianisotropic materials. Thus a complete understanding of the full properties of the SRRs must be taken to avoid ambiguities associated with absolute value measurements.

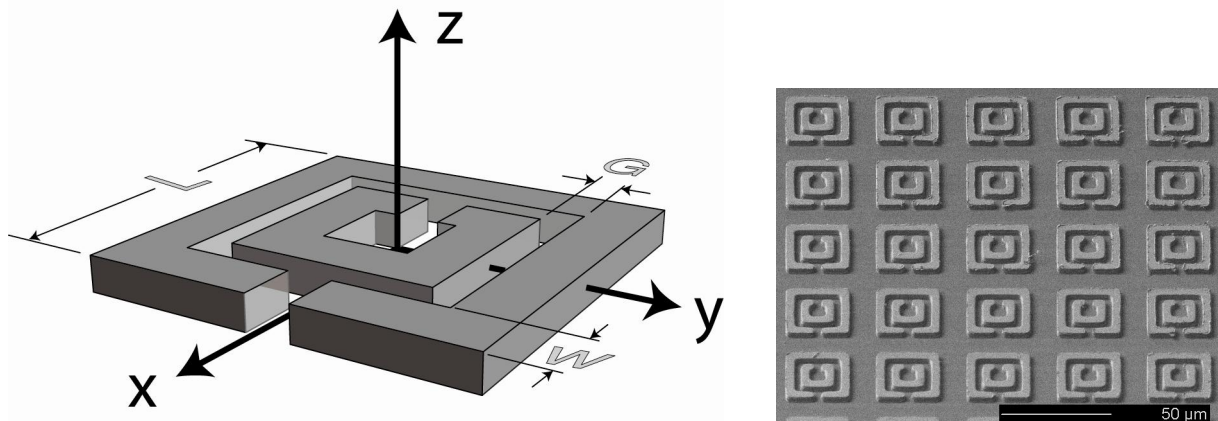


Figure 1: Left panel depicts the split ring resonator, where the black text labels the coordinate system, and the grey text labels the SRR dimensions. Right panel is a focused ion beam image of the SRR sample D1 made of 3μm thick copper elements on a 400μm quartz substrate.

We present a systematic study of three different SRRs fabricated for investigation of magnetic response in the THz or far infrared region of the electromagnetic spectrum. The samples are studied at room temperature in a reflection geometry experiment at oblique incidence. The magnetic response of SRRs at THz frequencies is demonstrated utilizing an ellipsometric approach.

Since it is known that the SRRs also exhibit an electric response, ellipsometry permits a straightforward way to extract the magnetic signal while minimizing the electric response. A 30° reflectance measurement was performed on three different SRR samples D1, D2, and D3. Each was designed to respond magnetically in the THz regime. An angle of 30° also permitted the overall dimensions of the sample to remain small thus facilitating fabrication of the SRRs.

The oblique reflectance measurement was performed with both P (transverse magnetic, TM) and S (transverse electric, TE) polarized light, as detailed in Table 1. SRR structures are bianisotropic,^{vii} thus additionally the samples were further characterized rotated by 90° in the sample plane, see Table 1. We introduce the notation symmetric and antisymmetric to distinguish between the orientation of the electric field vector being parallel and perpendicular to the split gaps of the SRR respectively, (left column of Table 1). This distinction is necessary because, for example, the main cause of chirality in artificial structures is the lack of a mirror symmetric geometry,^{viii} which is relevant for cases (C) and (D) of Table 1.

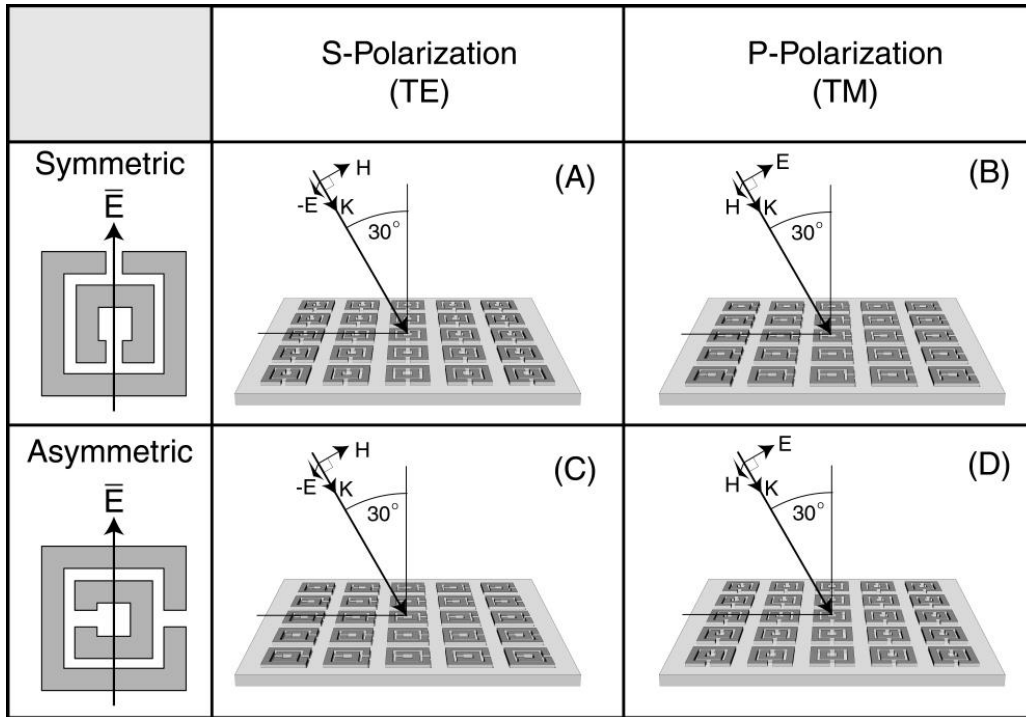


Table 1: Depiction of the four measurements completed for each SRR array sample. The left row headings denote the orientation of the electric field with respect to the split gaps and the top column headings refer to the state of the incident light upon the sample. Panel A shows the orientation in which a magnetic response is expected with a minimum contribution from the electric field, while in (B) no magnetic response is expected but a similar electric response is expected. The reflectance obtained from (A) is notated by R_S^{symm} and R_p^{symm} for (B). In panel C (R_S^{asymm}) although a magnetic response is predicted there should be a strong electric dipole response due to the asymmetric orientation of the electric field on the SRR. Finally in panel D (R_p^{asymm}) the SRRs should exhibit no magnetic but the same electric dipole response as in (C).

2. SAMPLE PREPARATION

The SRRs were made on a double-sided polished quartz substrate. A 5 μm thick negative photoresist (NR5-8000P, Futurrex Inc.) layer is spun onto the transparent quartz substrate, followed by a contact-mode lithographic process to transfer the designed SRR pattern as a mold. Then 10 nm of chromium followed by a 1 μm thick copper layer are deposited inside the mold by using a SLOAN SL 1800 e-beam evaporator. An acetone solvent rinse in an ultrasonic bath is then employed to remove the PR mold. This liftoff process results in a conductive non-magnetic layer patterned on the double-side polished quartz substrate.

Sample	Gap (G)	Width (W)	Side length (L)	Lattice Parameter (P)
D1	2	4	26	36
D2	3	4	32	44
D3	3	6	36	50

Table 2: Dimensions in microns of the SRRs characterized in this study. The single SRRs are the same dimensions as the double SRRs above, but without the inner ring. The split gap for all structure is 2 μm .

Another layer of photoresist is spun on top of the SRR structure for a second lithographic process. A flood exposure from the back side of the quartz substrate utilizes the SRR structures themselves serve as a mask for this lithographic process, and the exposure step is trouble-free since an external mask and an alignment step are not required. Finally, a

second copper evaporation and lift-off process are repeated in order to increase the thickness of the SRR structures. The right panel of Fig. 1 shows a secondary ion image of fabricated sample D1 taken under focused ion beam microscopy. The size of the die is 8 mm by 8 mm, and the dimensions of all samples characterized are listed in Table 2. Focused ion beam microscopy measurements indicate that the deviations of the fabricated sample dimensions from the designed values are less than 4% for all three samples. This deviation leads to no more than a 1% peak shift in the simulated response. Compared to the width of the peak (30%) this shift is negligible.

3. ELECTROMAGNETIC RESPONSE OF BIANISOTROIC MATERIALS

The constitutive relations for bianisotropic materials may be written as^{ix}:

$$\begin{bmatrix} \bar{D} \\ \bar{B} \end{bmatrix} = \begin{bmatrix} \bar{\epsilon} & \bar{\xi} \\ \bar{\zeta} & \bar{\mu} \end{bmatrix} \cdot \begin{bmatrix} \bar{E} \\ \bar{H} \end{bmatrix} \quad (1)$$

In Eq.1 the permittivities within the 2x2 matrix are, in general, tensors of second rank, also called dyadics. From this point on in the manuscript we explicitly write out the matrix components of the fields and response functions, thus the dyadic and vector notation will not be used unless necessary. For completeness we summarize in Table 4 the various materials definitions for different symmetry properties of the constitutive relations.

The terms ξ and ζ are called the magneto-optical permittivities, and they describe coupling of the magnetic to electric response and electric to magnetic response respectively. Then for the SRRs with the geometry specified in Fig. 1, and the expected bianisotropic nature, the constitutive relations are,

$$\bar{D} = \begin{bmatrix} \epsilon_{xx} & 0 & 0 \\ 0 & \epsilon_{yy} & 0 \\ 0 & 0 & 1 \end{bmatrix} \cdot \bar{E} + \begin{bmatrix} 0 & 0 & 0 \\ 0 & 0 & \xi_{yz} \\ 0 & 0 & 0 \end{bmatrix} \cdot \bar{H} \quad (2a)$$

$$\bar{B} = \begin{bmatrix} 0 & 0 & 0 \\ 0 & 0 & 0 \\ 0 & \zeta_{zy} & 0 \end{bmatrix} \cdot \bar{E} + \begin{bmatrix} 1 & 0 & 0 \\ 0 & 1 & 0 \\ 0 & 0 & \mu_{zz} \end{bmatrix} \cdot \bar{H} . \quad (2b)$$

As mentioned the particular geometry chosen is a 30° reflection experiment. The components of the incident electromagnetic field are worked out in Table 3 for all geometries characterized. The parallel and perpendicular components designated by (\parallel) and (\perp) are, for example, $H_{\parallel} = H_0 \cos(30)$ and $H_{\perp} = H_0 \sin(30)$.

	S-polarization	P-polarization
Symmetric	$\bar{E} = \begin{bmatrix} E_0 \\ 0 \\ 0 \end{bmatrix}, \bar{H} = \begin{bmatrix} 0 \\ H_{\parallel} \\ H_{\perp} \end{bmatrix}$	$\bar{E} = \begin{bmatrix} E_{\parallel} \\ 0 \\ E_{\perp} \end{bmatrix}, \bar{H} = \begin{bmatrix} 0 \\ H_0 \\ 0 \end{bmatrix}$
Asymmetric	$\bar{E} = \begin{bmatrix} 0 \\ E_0 \\ 0 \end{bmatrix}, \bar{H} = \begin{bmatrix} H_{\parallel} \\ 0 \\ H_{\perp} \end{bmatrix}$	$\bar{E} = \begin{bmatrix} 0 \\ E_{\parallel} \\ E_{\perp} \end{bmatrix}, \bar{H} = \begin{bmatrix} H_0 \\ 0 \\ 0 \end{bmatrix}$

Table 3. The components of the electric and magnetic incident radiation for the 30 degree reflectance measurement.

Thus the electric and magnetic contributions to the 30° reflectance measurements of the SRRs are given from Table 3 and equation 2 to be,

$$R_S^{symm} \rightarrow \mu_{zz} H_{\perp} + \epsilon_{xx} E_0 + \xi_{yz} H_{\perp} \quad (3a)$$

$$R_P^{symm} \rightarrow \epsilon_{xx} E_{\parallel} \quad (3b)$$

$$R_S^{asymm} \rightarrow \mu_{zz} H_{\perp} + \epsilon_{yy} E_0 + \xi_{yz} H_{\perp} + \zeta_{zy} E_0 \quad (3c)$$

$$R_P^{asymm} \rightarrow \epsilon_{yy} E_{\parallel} + \zeta_{zy} E_{\parallel}. \quad (3d)$$

Note that the above equations show the different contributions to the reflectance only, and not the actual form. The issue of computing an expression for the oblique incidence reflectance from a bianisotropic crystal is a complicated and tedious task, and may not be representable in a closed form. Analytical solutions may be obtained for various simple cases such as the reflectance from uniaxial crystals, which results in a modified form for the Fresnel equations.^x With considerably more effort the reflection and transmission coefficients can be worked out for anisotropic, bianisotropic, and anisotropic stratified media by the means of Berreman's 4 x 4 matrix method.^{xi} A similar and simpler method involves determination of the so-called Jones matrix.^{xii} The Jones matrix describes the polarization state of the incident electromagnetic radiation, in terms of S and P polarized light, and the changes this light undergoes upon reflectance from a sample at oblique incidence. This technique differs from Berreman's method in that the backward propagating equations within the media are ignored. These methods are very useful and often utilized in Variable Angle Spectroscopic Ellipsometry (VASE).^{xiii}

The magneto-optical permittivities may lead to more exotic electrodynamic behavior. For example in a simpler case, bi-isotropic media are commonly characterized through the chirality parameter (κ) and non-reciprocity or Tellegen parameter (χ). These are defined by,^{viii}

$$\kappa = \frac{i}{2\sqrt{\epsilon_0\mu_0}}(\xi - \zeta) \quad (4a)$$

$$\chi = \frac{1}{2\sqrt{\epsilon_0\mu_0}}(\xi + \zeta). \quad (4b)$$

We have looked extensively for non-reciprocal behavior due to the SRRs and have found none within the noise level of the measurements, ~1%. However, in general for SRRs it is expected that $\bar{\xi}$ and $\bar{\zeta}$ are non-zero in the vicinity of the resonant frequency.^{vii} Bianisotropic media is reciprocal if $\bar{\epsilon} = \bar{\epsilon}^T$ and $\bar{\mu} = \bar{\mu}^T$ and $\bar{\xi} = -\bar{\zeta}^T$, where T denotes the transpose. Thus if $\bar{\xi}$ and $\bar{\zeta}$ are non-zero and the SRRs are reciprocal media ($\xi_{yz} = -\zeta_{zy}$), then they may also be chiral. In fact due to the lack of reflection symmetry, depicted in Table 1C and D, theory predicts a chiral response. Signs of chirality should be observable by performing a crossed polarized experiment (i.e. polarimetry measurement); however we have been unable to find any indications of this cross polarization. Thus we neglect all of the magneto-optical permittivities for the symmetric case. For the asymmetric case notice that $\zeta \neq 0$ for both polarizations and $\zeta > \xi$ for S-polarization. Therefore we only consider ζ for the asymmetric case. With these assumptions and from Equations 3a-3d we have the following final contributions to the ellipsometric measurements displayed in Fig. 3:

$$\tan^{-2}(\Psi)_S^{symm} = \frac{R_S^{symm}}{R_P^{symm}} \rightarrow \frac{\mu_{zz} H_{\perp} + \epsilon_{xx} E_0}{\epsilon_{xx} E_{\parallel}} \quad (5a)$$

$$\tan^{-2}(\Psi)_S^{asymm} = \frac{R_S^{asymm}}{R_P^{asymm}} \rightarrow \frac{\mu_{zz} H_{\perp} + \epsilon_{yy} E_0 + \zeta_{zy} E_0}{\epsilon_{yy} E_{\parallel}} \quad (5b)$$

Lastly let us consider the qualitatively form for ϵ_{xx} and ϵ_{yy} . For a similar bianisotropic structure consisting of a random arrangement of metal helices embedded in a dielectric material, it was shown that if an electric field oriented along the axis excites the helices, charges are separated thus creating an electric dipole moment.^{viii} For our particular case, the SRRs would experience the same separation of charges, but only for a particular orientation of the electric field, which is the ϵ_{yy} case. In fact this has been worked out for SRRs in reference [vii]. The key result was that the for the ϵ_{xx} case the SRRs are expected to have a constant polarizability, taken to be that of a disk, whereas for the ϵ_{yy} case the SRRs

exhibit the same ϵ_{xx} polarizability plus a frequency dependent resonant dipole response. Since both an electric resonance and a magnetic resonance can be described with a Lorentizan oscillator, and moreover enter similarly in the Fresnel equations,^{xiv} it is difficult to distinguish between the two in either a reflection or transmission experiment at normal incidence. One might suppose that in order to discriminate between an ϵ and μ response that it would be sufficient to close the gap in the SRR, thus eliminating the resonant magnetic response. However in the asymmetric case this also removes the electric dipole response of the SRR, and hence this type of analysis is inconclusive. Thus the simplest way to avoid this ambiguity is to characterize the SRRs in the symmetric orientation so as to avoid the dipole electric resonance inherent to the asymmetric case.

Material designation	ϵ, μ	ξ, ζ
Isotropic	$\sim \mathbf{I}$	$\xi, \zeta = 0$
Anisotropic	ϵ and/or μ not $\sim \mathbf{I}$	$\xi, \zeta = 0$
Bi-Isotropic	$\sim \mathbf{I}$	$\sim \mathbf{I}$
Bi-Anisotropic	all other cases	all other cases

Table 4: Material classification with respect to the symmetry of constitutive relations. \mathbf{I} denotes the identity matrix.

4. SIMULATION

For analysis of the SRRs employed in this study, we have chosen the Jones matrix methodology. A software package, WVASE32, for the analysis of ellipsometric data, made by J.A. Woolam Inc. is utilized for the modeling of the oblique reflectance of S and P polarized light from the bianisotropic SRRs. The program has the ability to simulate oblique angle reflectances, given the complex electric and magnetic response.

The complex values $\tilde{\epsilon} = \epsilon_1 + i\epsilon_2$ and $\tilde{\mu} = \mu_1 + i\mu_2$ were obtained by a numerical simulation using High-Frequency Structure Simulator (HFSS), a commercial electromagnetic mode solver. The calculation was performed to determine the frequency dependent complex magnetic and electric response of the SRRs for use in the WVASE32 analysis software. S-parameter transmission and reflection were calculated as a function of frequency for a periodic infinite array of copper SRRs with the dimensions detailed in Table 2. In order to calculate μ_{zz} , ϵ_{xx} , and ϵ_{yy} , for input to the WVASE32 program, the propagation of the incident radiation was parallel to the plane of the SRRs (90° to the surface normal of Fig. 1). The electrical conductivity used for the copper elements was $\sigma = 5.8 \times 10^7$ S/m, and for the quartz substrate we used a dielectric constant of 3.78.

The effective frequency dependent magnetic permeability $\mu_{zz}(\omega)$ can be extracted from the S-parameter simulation results and used to calculate the expected theoretical reflectance ratio $\tan^{-2}(\Psi)$. This retrieval of the complex material parameters proceeds by a simulation of the frequency dependent transmission (\mathcal{S}_{21}) and reflection (\mathcal{S}_{11}) from a unit cell of the SRRs. For continuous isotropic materials, \mathcal{S}_{21} and \mathcal{S}_{11} have analytic forms that can be readily inverted.^{xv} The inversion of the scattering equations leads to the following form that allows determination of the refractive index (n) and impedance (Z):

$$\cos(nkd) = \operatorname{Re} \left(\frac{1}{\mathcal{S}_{21}} \right) - \frac{1}{2|\mathcal{S}_{21}|^2} (A_1 \mathcal{S}_{11} + A_2 \mathcal{S}_{21}) \quad (6a)$$

$$Z = \pm \sqrt{\frac{(1 + \mathcal{S}_{11})^2 - \mathcal{S}_{21}^2}{(1 - \mathcal{S}_{11})^2 - \mathcal{S}_{21}^2}} \quad (6b)$$

where A_1 and A_2 are real valued functions that tend to zero in the absence of losses.

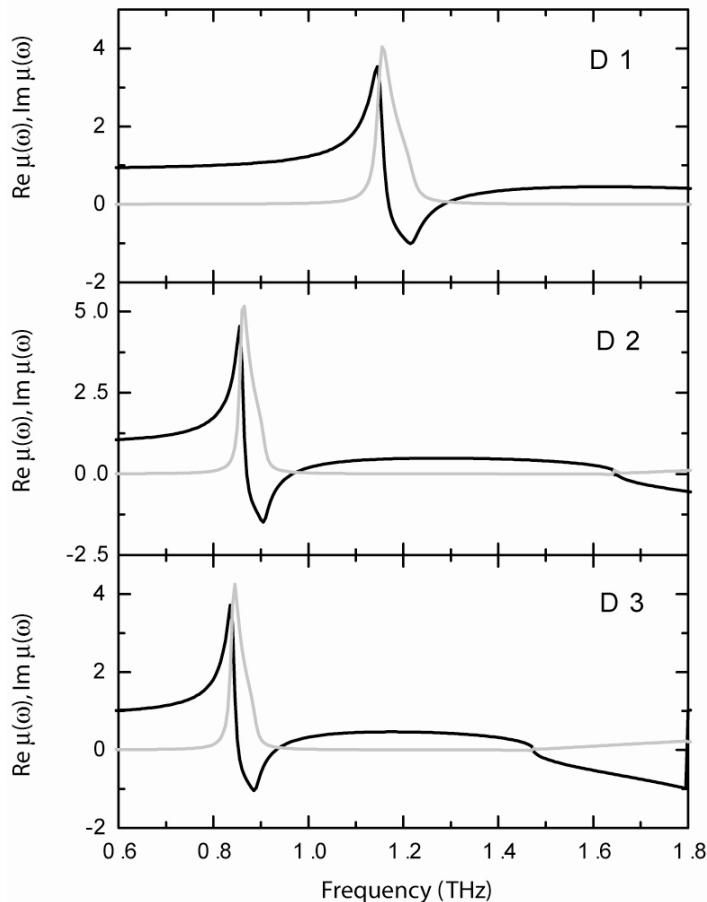


Figure 2: Simulation results for the three double SRRs. The real (black) and imaginary (grey) portions of the magnetic permeability are plotted for each sample as indicated. For each sample the simulation predicts a region of negative μ .

A retrieval procedure to determine the impedance and the index of refraction was carried out on the three SRRs. From Equation 6a notice that the retrieval of the index (n) is complicated by multiple branches due to the arccosine function. In our case the branches are sufficiently separated for the thin sample measured (one unit cell in thickness) so that no sophisticated retrieval algorithm was necessary. However there is a sign ambiguity between n and Z which can be eliminated by imposing causality, i.e. $\text{Re}(Z) > 0$ and $\text{Im}(n) > 0$.

5. ELLIPSOMETRIC RESULTS

Results from the oblique angle reflectance measurements are shown in Fig. 2. The top set of curves are for samples D1, D2, and D3 in the symmetric orientation, whereas the lower set of curves are for the same samples but in the asymmetric orientation.

As mentioned the SRRs characterized in this study have been designed to yield a magnetic response in the THz regime of the electromagnetic spectrum. This magnetic response is strongest when the incident magnetic field is parallel to μ_{zz} . At infrared frequencies the planar SRR structures would then require a grazing incidence measurement for maximum magnetic coupling. However, to ease sample fabrication a 30° reflectance measurement provides suitable magnetic coupling while keeping dimensions relatively small.

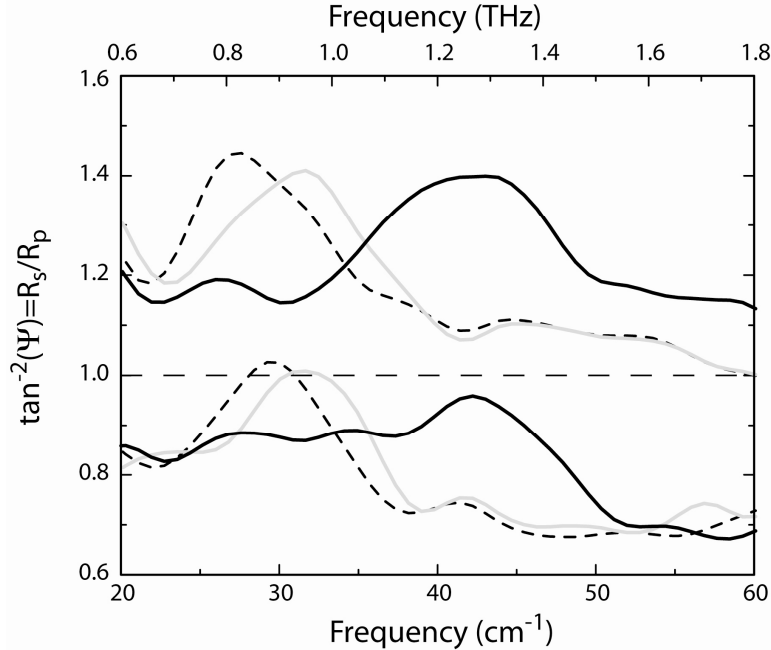


Figure 3: Magnetic response from samples D1, D2, and D3 determined in two different ways. The top set of curves is determined in the symmetric orientation and the bottom set of curves, the asymmetric orientation, where symmetric and asymmetric are defined in the text.

The symmetric magnet response from sample D1, (upper solid black curve of Fig. 2), exhibits a broad maximum centered at approximately 1.25 THz and is otherwise relatively frequency independent. As we scale the dimensions of the SRRs larger the peak maximum can be observed to shift to lower frequencies, in accord with Maxwell's equations. The parameter plotted $\tan^2(\Psi)$ is related to the well known ellipsometric parameter $\rho(\omega)$ by,

$$\rho = \frac{r_p}{r_s} = \tan(\Psi)e^{i\Delta}. \quad (7)$$

Where we use the usual definition $R_p = |r_p|^2$. As mentioned the SRRs exhibit a magnetic response for excitation with S-polarized light. For P-polarized light the magnetic component lies entirely within the plane of the sample and thus a magnetic response is not expected. However there is, as previously mentioned, an electric response. Therefore the parameter R_s/R_p represents the magnetic response normalized by the electric response of the SRRs.

Although the ratio of two absolute value reflectances may be related to well known ellipsometric terms, one must be cautious in the interpretation of the data. For example, examination of Equation 5a, in the symmetric case predicts frequency dependent behavior solely from the resonant magnetic response of the SRRs. Thus the set of curves should all lie at $\tan^2(\Psi) \sim 1.15$, since $\epsilon_{xx} \neq \epsilon_{xx}(\omega)$ and $E_0/E_{\parallel} = 1/\cos(30)$, and only deviates to greater values for a magnetic response. Thus we see that Equation 5a is a suitable representation for the symmetric response and R_s^{symm} and R_p^{symm} may be simply described by the ordinary Fresnel equations with Lorentzian $\mu_{xx}(\omega)$ and constant ϵ_{xx} contributions.

For the more complicated asymmetric case notice all values for $\tan^2(\Psi)$ are significantly less than 1. This is because in addition to the symmetric case we also have a resonant electric response $\epsilon_{yy} = \epsilon_{yy}(\omega)$, as well as a non-negligible

frequency dependent cross coupling, i.e. $\zeta_{zy} \neq 0$. Thus the analysis is complex and we do not elaborate on this further.

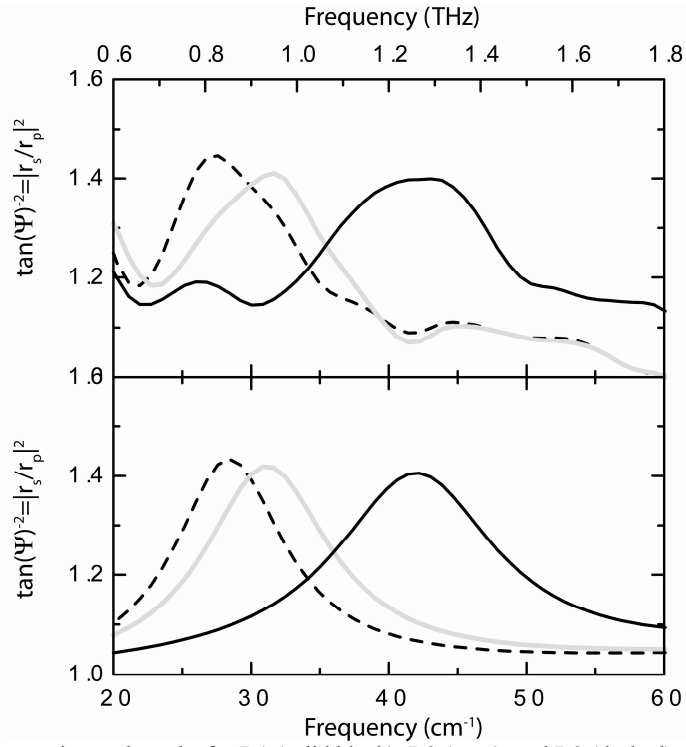


Figure 3: Comparison of the experimental results for D1 (solid black), D2 (grey), and D3 (dashed) to the simulated response for the same structures. The input to simulation was the exact dimensions of each SRR as detailed in Table 2.

6. DISCUSSION

It is interesting to consider the effects of bianisotropy on negative index behavior and whether or not these effects are detrimental or beneficial in this regard. Theoretical investigations of periodic chiral media demonstrated significantly richer band-gap structure than their achiral counterparts.^{xvi} More generally the index of refraction was worked out for electromagnetic wave propagation in stratified bi-isotropic media and shown to be,^{xvii}

$$n_{\pm} = \sqrt{\epsilon\mu - \chi^2} \pm \kappa \tag{8}$$

where the (+) and (-) signs corresponds to left and right circularly polarized light respectively, and the non-reciprocal and chiral parameters are defined in Equations 4(a) and 4(b). It was noted in ref.[xvii] that for $n_{\pm} > 0$ waves travel in the forward direction, and backward for $n_{\pm} < 0$. Thus we may conclude that for bi-isotropic materials and certain polarizations, a negative index band can still be constructed utilizing chirality as prescribed by Equations (8) and (4a). More importantly notice that irrespective of polarization, non-reciprocity is always beneficial towards achieving negative index independent of the values of the permittivity and permeability.

The constitutive relations for bianisotropic SRRs is more complicated than the bi-isotropic case but we can expect a similar enhancement of the band structure as well as an effect on negative index. In general since the SRRs are chiral then the same dependence of NI on polarization is expected and this has recently shown.^{xviii}

7. CONCLUSIONS

We have shown measurements of three different SRR samples all at THz frequencies. The theoretical response has been calculated using a combination of eigenmode simulation and Jones matrix methodology. The SRRs respond magnetically, but have an electric response which cannot be neglected in the analysis. Simulation predicts a frequency dependent magnetic response for each SRR and indicates a region where $\mu(\omega)$ obtains negative values. We find a good agreement between experiment and theory for all samples in the symmetric orientation. This demonstrates that although the SRR materials are inherently bianisotropic, it is suitable to describe their response by neglecting the magneto-optical permittivities in the symmetric case.

On the other hand we have demonstrated that two issues complicate the response of the SRRs in the asymmetric orientation. First the SRRs are chiral in this orientation and thus the magneto-optical permittivities cannot be ignored. Secondly and more significantly, the SRRs exhibit a strong frequency dependent electric dipole response in the asymmetric orientation which overwhelms the magnetic response. Further, the electric and magnetic resonances occur at roughly the same frequency. Simulation (not shown) indicates that this electric resonance has an oscillator strength that is 50 times greater than the magnetic response and thus dominates absolute value spectra. As an added confusion, simply closing the gap in the SRRs is inconclusive because this eliminates both the chirality and the electric dipole response. Thus one has to be very wary when analyzing reflectance or transmission spectra since both magnetic and electric response enter mixed, complicating the analysis.

Due to the lack of routine complex measurements at THz and higher frequencies along with the added difficulty of fabricating ever smaller SRR structures, one must be aware of the inherent bianisotropic nature of structures utilized for achieving magnetic response. It has been shown that through careful analysis, it is possible to demonstrate and prove magnetic response, although many pitfalls exist.

REFERENCES

-
- ⁱ. D. R. Smith, W. J. Padilla, D. C. Vier, S. C. Nemat-Nasser, S. Schultz, *Phys. Rev. Lett.* **84**, 4184 (2000).
 - ⁱⁱ. V. G. Veselago, *Soviet Physics USPEKI* **10**, 509 (1968).
 - ⁱⁱⁱ. T. J. Yen, W. J. Padilla, N. Fang, D. C. Vier, D. R. Smith, J. B. Pendry, D. N. Basov, and X. Zhang, *Science* **303**, 1494 (2004).
 - ^{iv}. J. B. Pendry, A. J. Holden, D. J. Robbins, and W. J. Stewart, *IEEE Trans. Microwave Theory Tech.* **47**, 2075 (1999).
 - ^v. M.C.K. Wiltshire, J.B. Pendry, I.R. Young, D.J. Larkman, D.J. Gilderdale, and J.V. Hajnal, *Science* **291**, 849 (2001).
 - ^{vi}. J.B. Pendry, D.R. Smith, *Physics Today* **57** (6), 37 (2004).
 - ^{vii}. R. Marques, F. Medina, R. Rafii-El-Idrissi, *Phys. Rev. B* **65**, 144440 (2002).
 - ^{viii}. I.V. Lindell, A.H. Sihvola, S.A. Tretyakov, A.J. Viitanen, *Electromagnetic Waves in Chiral and Bi-Isotropic Media* (Artech House Inc., London, 1994).
 - ^{ix}. J.A. Kong, *Electromagnetic Wave Theory* (John Wiley & Sons, Inc., New York, 1990).
 - ^x. L.P. Mosteller, Jr., F. Wooten, *J. Opt. Soc. Am.* **58**, 511 (1968).
 - ^{xi}. D.W. Berreman, *J. Opt. Soc. Am.* **62**, 502 (1971).
 - ^{xii}. R.C. Jones, *J. Opt. Soc. Am.* **31**, 488 (1941); **32**, 486 (1942).
 - ^{xiii}. R. M. A. Azzam and N. M. Bashara, *Ellipsometry And Polarized Light* (Elsevier, New York, 1999).
 - ^{xiv}. In the Fresnel equations (neglecting the magneto-optical permittivities), for reflectance of oscillators of equal strength at oblique incidence the S-polarized reflectance is greater than the P-polarized reflectance for an electric resonance, whereas the opposite is true for a magnetic resonance. Thus it is possible to distinguish between an electric and magnetic response by completing an oblique incidence reflectance measurement.
 - ^{xv}. D. R. Smith, S. Schultz, P. Markos, and C. M. Soukoulis, *Phys. Rev. B* **65**, 195104 (2002).
 - ^{xvi}. K. M. Flood, D. L. Jaggard, *J. Opt. Soc. Am. A* **13**, 1395 (1996).
 - ^{xvii}. O. V. Ivanov, D. I. Sementsov, *Crystallography Reports* **45**, 487 (2000).
 - ^{xviii}. J.B. Pendry, *Science* **306**, 1353 (2004).